

Selection of Capacitance for Compensated Self Excited Induction Generator Using Meta-Heuristic Approach

Radwan M. AL- Bouthigy

Electrical Engineering Department, Faculty of Engineering, Sana'a University, Yemen

Email address: r.albouthigy@eng-su.academy

Abstract— The performance of self-excited induction generator was thoroughly analyzed regarding the values of the critical excitation capacitance and the frequency of the generated voltage. Analytical expressions were derived for the value of the minimum excitation capacitor under different load types/operating conditions. The advised expressions were verified experimentally and by, a robust meta-heuristic optimization technique, particle Swarm Algorithm. Furthermore, the feasibility, suitability and effectiveness. of the proposed formulas were corroborated for generators with different sizes/ratings through the correlation of the results from the derived expressions and Particle Swarm Algorithm for such machines.

Keywords— Self Excitation, induction generator, particle swarm algorithm, critical capacitance, magnetizing reactance.

I. INTRODUCTION

Induction Generator (IG) is the preferred option for harnessing electrical power from non-conventional energy sources, particularly wind. This is attributed to the salient features of IG such as: robustness, maintenance free, short-circuit protection capability and absence of separate DC excitation system [1-3]. IG could be operated either grid-connected or off-line; for the case of grid-connected, the reactive power requirements for maintaining constant voltage at generator terminals under different load/speed conditions are supplied by the grid. However, for the case of stand-alone operation, which is the case for remote and rural locations, the capacitive excitation is indispensable to regulate the voltage across the machine terminals [3-7].

The machine terminal voltage decreases/increases with the load increase/reduction for fixed excitation capacitance and constant speed operation. To regulate the terminal voltage, the excitation capacitance has to vary simultaneously with the load. This is a costly and complicated solution. However, if the terminal voltage is allowed to vary within a narrow range, an attractive, in-expensive and simple approach is to use stepped switched capacitors with the possibility of switching them on/off with the loads [3-5].

The principle of self-excitation was employed in other research areas as dynamic braking of three-phase induction motor; therefore, the techniques for analyzing the behavior of such machines are of significant practical interest [3], [5]. In general, there are two scenarios for analyzing the steady-state performance of self-excited cage induction generator. The first scenario is to determine terminal voltage, output power, stator

and rotor currents for given values of capacitance, load and speed, while the second is to determine the required excitation capacitance for the desired voltage at given load and speed levels [7-21].

Extensive research efforts were drafted in the past decades [5-11] for investigating the steady state performance of Self Excited IG (SEIG) using the steady-state equivalent circuit. For example, [1] exposes in Section 19.4 a second order slip equation. It was obtained from the steady-state equivalent circuit. This equation, as claimed in [1], could predict the occurrence of self-excitation in SEIG through examining the roots of the advised equation. However, the numerical values for all the SEIG parameters including resistance, generated frequency, excitation capacitive, magnetizing and leakage reactance's should be supplied to solve this equation. Thus, this equation could not identify explicitly, which parameters affect self-excitation process. Moreover, [1] introduces no validation for such equation either from simulation or experimental work.

A mathematical model in [8], [9] was developed for obtaining the steady state performance of SEIG using the equivalent circuit. In this approach, the complex impedance is segregated into real and imaginary parts. The resulted nonlinear equations are arranged for unknown variables such as magnetizing reactance (X_m) and frequency (F), while the remaining machine parameters and operating variables are assumed constants. Numerical techniques as Newton Raphson were employed for solving the equations. This approach, however, requires sophisticated computation capabilities in terms of speed and storage. In [10] an approach for computing steady state performance of the self-excited induction generator is proposed; 4th order polynomial is derived from the loop equation of the equivalent circuit of the machine. The roots of this polynomial are determined to check occurrence of self-excitation and to get the corresponding value of magnetizing reactance. The approach proposed in [10] has the advantage of predicting the performance of the machine for given capacitance/load/speed level. However, the load considered in this approach is pure resistive, which has less practical significance.

A mathematical formula was proposed in [11] based on steady state equivalent circuit of the machine for computing the minimum value of the capacitance required for self-excitation and the threshold speed, below which self-excitation could not be established. Another mathematical

formula is proposed in [12] for computing the static performance of the induction generator under wide range of operating conditions. In [13-15], the performance of separate-excited induction generator is investigated to evaluate the range of different parameters as voltage, speed and excitation capacitance, within which self-excitation is possible.

In [16] an analysis for the performance of SEIG based on eigenvalues is proposed. The lower and upper limits of the excitation capacitance are identified. However, this approach is a numerical iterative procedure. The computation time and speed rely on the initial guess, which is inconvenient. Moreover, the distinction between the value of minimum and maximum capacitance is only the value of the initial guess, either it is small or large. This limits the proposed method applicability for machines with specific rating [16]. The critical capacitance under different load conditions was predicted using simulated annealing optimization technique in [17]. However, the rotor speed is restricted within a narrow range. The relation between the excitation capacitance and the machine parameters and load types could not be visualized. Moreover, there is no experimental collaboration for the analysis in [17].

Most of the reported approaches for evaluation of the steady-state performance of self-excited cage induction generators require splitting the equivalent impedance into real and imaginary components. Moreover, the model becomes rather complicated, if the core losses are included. Accordingly, several assumptions are taken to simplify the analysis. Furthermore, different models are used for modeling the machine with different types of loads/excitation capacitor arrangements. The coefficients of the mathematical models vary, which complicate the problem even further. Moreover, the derived mathematical formulas are only obtained for less practical loading condition, as resistive loads [8-21].

In this paper, analytical expressions were derived for the value of the critical capacitance under different load types/speed levels. Moreover, the value of the frequency of the generated voltage under different operating conditions is identified. The factors that affected the frequency of the generated voltage are addressed. The advantages of the derived analytical expressions here in this work are:

1. Identifying explicitly the machine parameters that affect the values of the excitation capacitor and generated frequency compared with the blind answers of the numerical methods.
2. Applicability for an arbitrary induction machine irrespective to rating, while numerical techniques are usually applied for a specific machine.
3. Addressing different operating/loading conditions as open-circuit, resistive and inductive loads, which as far as we know were not reported.

A meta-heuristics technique, Particle Swarm Algorithm (PSO) is employed for verifying the derived analytical expressions. The PSO uses a generic mathematic model for SEIG; this model is used for any load type/excitation capacitor arrangement. In PSO, the complex impedance is formulated as the objective function; and capacitive reactance and frequency

are taken as independent variables. The upper/lower limits of the unknown variables are selected to achieve practically acceptable values. The results from PSO technique are used for verifying the derived analytical expression under different load/speed levels. Furthermore, the derived expressions are experimentally collaborated.

II. CRITICAL EXCITATION CAPACITANCE

The following analysis is valid for SEIG, whether squirrel-cage or wound rotor, provided that the self-excitation arrangements are allocated in the stator side. The equivalent circuit of SEIG is shown in figure 1.

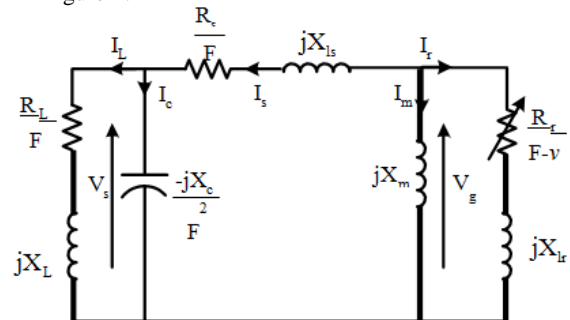


Fig. 1. Equivalent circuit of self-excited induction generator

$R_s, R_r, X_{Ls}, X_{Lr}, X_m, X_c, R_L$ and X_L are per phase stator resistance, rotor resistance, stator leakage reactance, rotor leakage reactance, magnetizing reactance, excitation capacitive reactance, load resistance and reactance respectively. The reactances in the equivalent circuit are calculated at base frequency. F and v are p.u. frequency and speed. I_s, I_r, I_m, I_c and I_L are per phase stator, rotor, magnetizing, capacitor and load currents respectively. The resistance, reactance, current and voltage of the rotor are referred to the stator. Applying loop-impedance method [14] in the equivalent circuit, Figure 1, the following equation results,

$$Z_T I_s = 0 \tag{1}$$

under steady-state self-excitation, $I_s \neq 0$, thus Z_T in (1) is equal to zero. Z_T is given by,

$$Z_T = Z_C Z_L (Z_M + Z_R) + Z_S (Z_M + Z_R)(Z_L + Z_C) + Z_M Z_R (Z_L + Z_C) \tag{2}$$

Where Z_s, Z_r, Z_m and Z_c are stator, rotor, magnetizing, excitation capacitance impedances respectively; they are given in Appendix. Equation (2) is used for investigating different load conditions in the following sections.

A. No-Load $Z_L = \infty$

The no-load operation of the SEIG is stimulated by equating load impedance by infinity $Z_L = \infty$. Substituting the values of

Z_s, Z_r, Z_m, Z_L and Z_c into (2) and equating the real and imaginary parts by zero; the value of the critical capacitive reactance is obtained for the no-load condition as,

$$X_{c-critical} = \left(\frac{R_s}{F} + \frac{R_r}{F-v} \right) (X_1 + X_m) \frac{F^2 (F-v)}{R_r} \tag{3}$$

and the frequency of the generated voltage is obtained from,

$$(2X_1X_m + X_1^2)F^3 - v(2X_1X_m + X_1^2)F^2 - (X_c(X_m + X_1) + R_sR_r)F + vX_c(X_m + X_1) = 0 \quad (4)$$

In no-load operation of SEIG, the machine slip is almost zero, and the pu frequency of the generated voltage is nearly equal to the pu rotor speed. Thus, substituting $F \approx v$ and setting $F-v \approx 0$ in (3), the critical capacitive reactance could be

$$X_{c-critical} \approx (X_1 + X_m)v^2 \quad (5)$$

Equation (5) indicates that minimum excitation capacitance is inversely proportional with square of rotor speed, leakage and magnetizing reactance's. Thus, the excitation capacitance has to fulfill the machine reactive power requirement for successful operation (5). Equation (5) coincides with conclusions in Section 19.6 in [1]. Equation (4) has three roots; two of these roots are discarded due to their extraordinary values. Thus, third root depicts the frequency. The frequency of the generated voltage was found to be independent of the leakage reactance, and it is speed dependent.

B. Resistive load $Z_L = \frac{R_L}{F}$

The critical capacitance for the resistive load case could be obtained by equating load impedance by $Z_L = \frac{R_L}{F}$; then

Substituting the values of Z_s, Z_r, Z_m, Z_L and Z_c into (2) and equating the real and imaginary parts by zero. The value of the critical capacitive reactance for resistive load case is given by,

$$X_{c-critical} = \frac{R_L \left(\frac{R_s}{F^2} + \frac{R_r}{F(F-v)} \right) (X_1 + X_m)}{\frac{R_r R}{F^3(F-v)} + \frac{R_r R}{F^3(F-v)} - \frac{2X_1X_m + X_1^2}{F^2}} \quad (6)$$

and the frequency of the generated voltage is obtained from,

$$R_L(2X_1X_m + X_1^2)F^3 - vR_L(2X_1X_m + X_1^2)F^2 - (X_c(X_m + X_1)(R_L + R_s + R_r) + R_sR_rR_L)F + vX_c(X_m + X_1)(R_L + R_s) = 0 \quad (7)$$

Equation (6) indicates that the critical capacitance is load dependent. Again, it varies with rotor speed and leakage and magnetizing reactance's. Similarly to (4), equation (7) has three roots; two of them are ignored, while the third provides the frequency of the generated voltage. The frequency is found to be a function in load resistance and machine speed, which concurs with the slip equation advised in [1].

C. Inductive Load $Z_L = \frac{R_L}{F} + jX$

Inductive load represents the generic case for the SEIG.

The load impedance is given by, $Z_L = \frac{R_L}{F} + jX$ Substituting the values of Z_s, Z_r, Z_m, Z_L and Z_c into (2) and equating the real and imaginary parts by zero; the value of the critical capacitive reactance for inductive load,

$$X_{c-critical} = \frac{R_L \left(\frac{R_s}{F^2} + \frac{R_r}{F(F-v)} \right) (X_1 + X_m) - (2X_1X_m + X_1^2)X_L + \frac{R_sR_rX_L}{F(F-v)}}{\frac{R_r R}{F^3(F-v)} + \frac{R_r R}{F^3(F-v)} - \frac{2X_1X_m + X_1^2}{F^2} - \frac{X_L(X_1 + X_m)}{F^2}} \quad (8)$$

and the frequency of the generated voltage is obtained from,

$$R_L(2X_1X_m + X_1^2)X_L(2X_1X_m + X_1^2)F^3 - v(R_L(2X_1X_m + X_1^2) + XR_s(X_m + X_1))F^2 - (X_c(X_m + X_1)(R_L + R_s + R_r) + R_sR_rR_L + X_cR_rX_L)F + vX_c(X_m + X_1)(R_L + R_s) = 0 \quad (9)$$

Equation (8) depicts clearly the relation between the excitation capacitance and load reactive power requirements, which are represented in load inductive reactance X_L . Again, the critical capacitive reactance varies with the prime mover speed and leakage and magnetizing reactance. Equation (9) has three roots similarly to (4) and (7), only one of these roots has acceptable value. Accordingly, the frequency of the generated voltage is found to be independent on leakage reactance; however it varies with the load, speed and motor copper losses.

III. PERFORMANCE OPTIMIZATION

For optimizing the performance of SEIG regarding the minimum capacitance and the corresponding generated frequency for given speed and load levels, the problem is mathematically formulated as,

$$\text{Minimize } |Z(F, X_c)| \quad (10)$$

Usually the frequency and capacitive reactance are bounded to reduce the computation time. This approach is used to verify the analytical results in (3)-(9). To fulfill (10), Z_T has to be segregated into real and imaginary parts; accordingly two nonlinear equations are obtained with X_c and F as unknown variables,

$$f(F, X_c) = a_1F^3 + a_2F + (a_3X_c + a_4)F + (a_5X_c) \quad (11)$$

$$g(F, X_c) = b_1F^4 + b_2F^3 + (b_3X_c + b_4)F^2 + (X_cb_5 + b_6)F + (b_7X_c) \quad (12)$$

where the coefficients a_1 - a_5 and b_1 - b_7 are given in the Appendix .

A. Particle Swarm Algorithms

The PSO method is a member of wide category of Swarm Intelligence methods for solving the optimization problems. It is a population based search algorithm where each individual is referred to as particle and represents a candidate solution. Each particle in PSO flies through the search space with an adaptable velocity that is dynamically modified according to its own flying experience and also the flying experience of the other particles [22]. The principle and mechanism of PSO are adequately covered in optimization references as [22]. The PSO was selected here in this work due to its relevant features, which are:

1. The capability of searching many points in the search space simultaneously,
2. The independency on the starting point(the initial solution is generated randomly),

3. Minimum requirements, as it needs only objective function and fitness function to modify and direct its performance,
4. Stochastic search method, which implies that the probability contributes to the most of the decisions.

IV. STUDY CASE

A delta connected 415V, 3.7kW SEIG is used for validating the derived expressions. The machine parameters are shown in Table I. X_m , the magnetizing reactance is determined experimentally through driving the machine at synchronous speed by a DC motor. The input frequency is kept at base value; while the input voltage is allowed to vary. The input impedance per-phase is calculated for different input voltage, to estimated the value for X_m . The drop in the stator impedance is taken into consideration in calculating air-gap voltage V_g . The magnetizing reactance is shown in the figure 2.

TABLE I. Parameters of 3.7KW IG

Number of poles	4
Frequency	50Hz
Stator resistance R_s (p.u.)	0.053 p.u
Rotor resistance referred to the stator R_r (p.u)	0.061 p.u
Stator leakage reactance X_{Ls} (p.u)	0.087 p.u
Rotor resistance referred to the stator X_{Lr} (p.u)	0.087 p.u

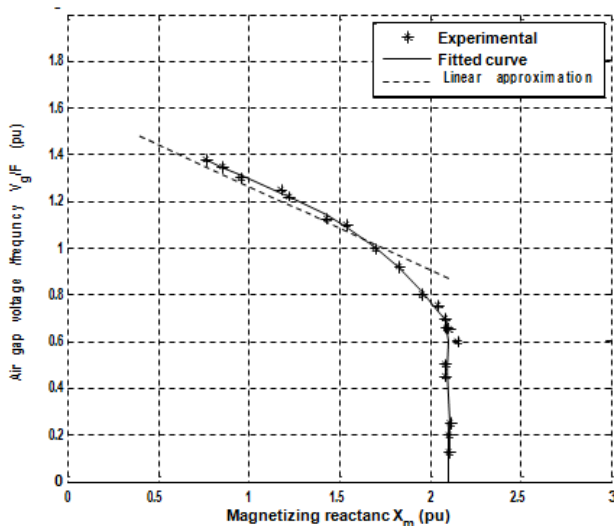


Fig. 2. Air gap voltage-frequency ratio (V_g/F) versus the magnetizing reactance X_m , experimental data (asterisk), fitted curve (solid), linear approximation (dashed)

The saturated magnetizing reactance is approximate by,

$$\frac{V_g}{F} = 1.62 - 0.32X_m \tag{13}$$

This approximation as shown in figure 2 correlates with the experimentally and the fitted data. To corroborate the derived expressions (3)-(8), a program is written in Matlab M-code for implementing PSO using PSO toolbox fitted in Matlab. The maximum number of generation is limited to 20, as compromise between accuracy and computation time. The objective function for PSO is obtained from (11) and (12). It is

implemented as a Matlab function that accepts the machine and load parameters, and it returns a minimum value of the amplitude of Z_T at a given frequency and capacitive reactance. Moreover, the analytical formulas were corroborated experimentally.

The steady-state performance of machine under concern was evaluated for different levels of excitation capacitance in the following sections.

V. STUDY-STATE PERFORMANCE

To evaluate the steady-state performance of the IG, the value of magnetizing reactance X_m and the generated voltage has to be determined for given speed, load and excitation capacitance. The magnetizing reactance X_m could possibly be computed under these conditions using PSO, and hence the mathematical formulation of the problem is given by,

$$\text{Minimize } |Z(F, X_m)| \tag{14}$$

The frequency and magnetizing reactance are bounded. To fulfill (14), Z_T again has to be segregated into real and imaginary parts; accordingly two nonlinear equations are obtained with X_m and F as unknown variables,

$$U(X_m, F) = F(c_1X_m + c_2) + F^2(c_3X_m + c_4) + F(c_5X_m + c_6) + (c_7X_m + c_8) \tag{15}$$

$$W(X_m, F) = F(d_1X_m + d_2) + F^3(d_3X_m + d_4) + F^2(d_5X_m + d_6) + F(d_7X_m + d_8) + d_9 \tag{16}$$

where the coefficients c_1 - c_8 and d_1 - d_9 are given in the Appendix .

To determine the minimum X_m for the given condition, a program coding PSO is written in Matlab environment. After determining the value of magnetizing reactance X_m and frequency F for given capacitance, speed, and load, the generated voltage V_g could be obtained from figure 2. Then, the load voltage, current and power could be obtained using the equivalent circuit by,

$$\left. \begin{aligned} I_L &= \frac{(V/F) * Z_c}{(Z_s + Z_L // Z_c)(Z_c + Z_L)} \\ V_L &= Z_L * I_L \\ P_L &= m |I_L|^2 R_L \end{aligned} \right\} \tag{17}$$

where the number of phases m for the machine under concern is 3.

VI. RESULTS AND DISCUSSIONS

The variation of the minimum capacitance and generated frequency with rotor speed for different operating scenarios are shown in figure 3 and figure 4 respectively. A good correlation is shown in figure 3 between the results from test-ring, optimization technique and equations (3)-(8). The values of threshold excitation capacitance from test-ring are slightly higher than those from PSO and analytical expressions. This attributed to the leakage, harmonics and parasitic inductances. Figure 3 shows that the critical capacitance for inductive load is significantly higher than that of resistive load and no-load.

This is attributed to the fact the excitation capacitor has to satisfy the reactive power requirements for the load and the generator simultaneously. Accordingly, capacitive load may require less capacitance than no-load case. The results in figure 3 coincide with conclusion in Section 19.6 in [1], particularly for no-load condition.

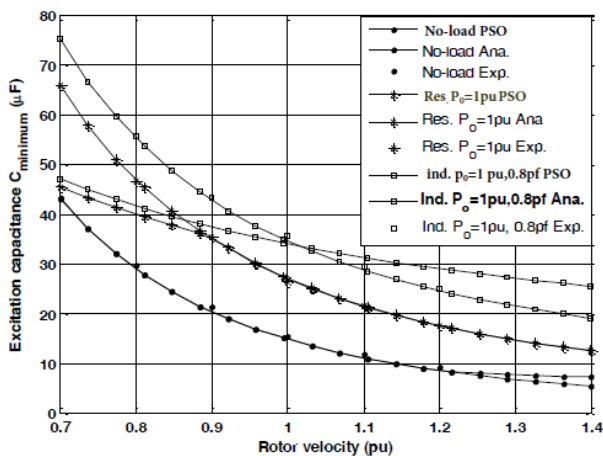


Fig. 3. Critical capacitance versus rotor speed for No-load (dots), resistive load at rated power (stars), inductive load at rated power and 0.8pf lag (squares) from analytical expressions (dashed line), PSO (solid line) and experimental (no line) for 3.7kW machine

The critical capacitance is a speed dependent, figure 3; the capacitance drops nearly by 40% for 25% increase in the speed. In figure 3, the deviation between the results from optimization and from the derived equations is attributed to the limits imposed on independent variables.

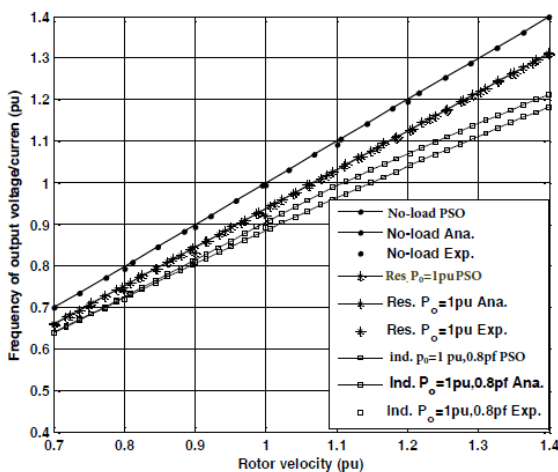


Fig. 4. Generated frequency versus rotor speed for No-load (dots), resistive load at rated power (stars), inductive load at rated power and 0.8pf lag (squares) from analytical expressions (dashed line), PSO (solid line) and experimental (no line)

The generated frequency from analytical expressions generally correlates with those from PSO and test-rig, figure 4; however, the results from optimizations for inductive load deviate from experimental and derived equations. This is attributed to the limits imposed on the PSO. The machine under consideration has large rotor resistance, Table I; thus the

slip at maximum developed power is approximately 0.35; which could explain the raised values of slip at other operating points. In case of no-load, the generated frequency almost is rotor velocity dependent.

The dependency of the generated voltage on excitation capacitor is exploited in figure 5 for three levels of rotor speed. The generated voltage shown in figure 5 is computed using steady-state equations and measured from the test-rig. In the test-rig, the terminal voltage and stator current are measured; then the generated voltage is obtained by subtracting the drop in stator impedance from the measured terminal voltage.

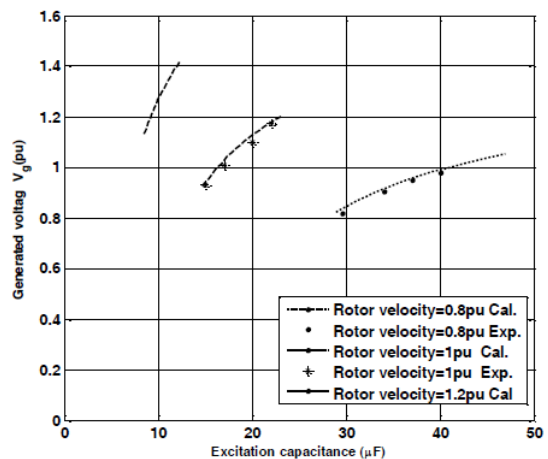


Fig. 5. Generated voltage versus capacitance at no load at 0.8pu rotor velocity (dots), 1pu rotor velocity (stars), 1.2pu rotor velocity (squares), calculation (solid line) and experimental (no line)

Again good corroboration between the computed and experimental results is shown in figure 5. The minimum capacitance required to ensure successful build up increases as the speed decreases. The generated voltage from the test-rig is slightly lower than the computed. This is attributed to saturation, core losses and drop in stator circuit. Figure 3 shows that for 3.7kW, 15µf is the minimum value of the excitation capacitance at rated speed, below which the self-excitation is not possible. Moreover, the Figure shows that there is upper limit for the excitation capacitor above which the machine reverts into saturation. In the saturation the increase in the excitation capacitance will not produce significant increase in output power/generated voltage, which could not overwhelm the increase in capacitor size, cost and losses.

The variations of the terminal voltage with output power for different levels of excitation capacitance are shown in figure 6 for resistive and inductive load at 0.8 pf lag types. The terminal voltage/output power of IG increases/decreases with increase/decrease in the excitation capacitance, figure 6, provided that saturation is not reached. Figure 6 shows that the voltage regulation for the inductive load is inferior compared to that of the resistive load; this may be attributed to the function of the excitation capacitor in case of inductive load in fulfilling the reactive power requirements of the load and the generator. It is observed from figure 6, that the characteristic

of self-excited induction generator is nearly similar to that of separately-excited DC generator.

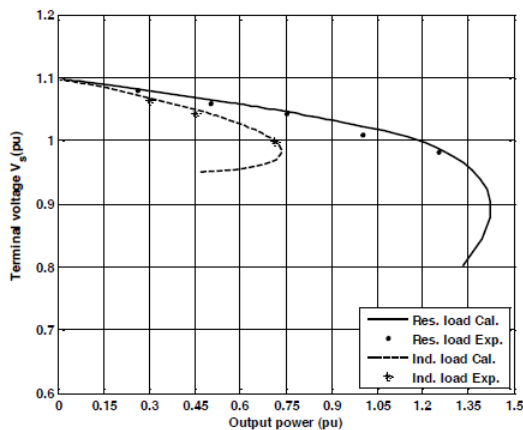


Fig. 6. Terminal voltage versus output power at rated speed and 29.6µF capacitor for pure resistive load: calculated (solid), experimental (dots); inductive load, 0.8pf lag calculated (dashed), experimental (stars)

The dependency of the output power on the excitation capacitance is exploited in figure 7, where the output powers are plotted versus the capacitance for constant terminal voltage/speed.

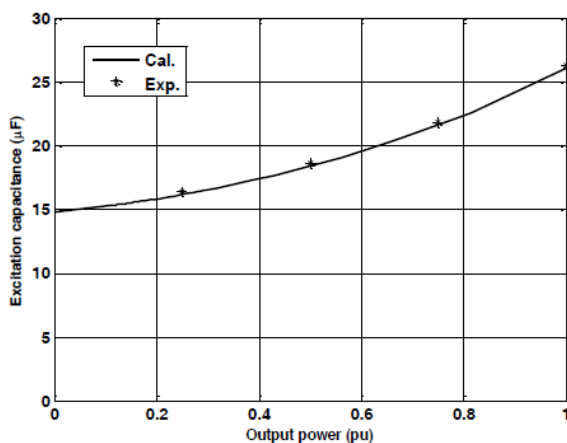


Fig. 7. Excitation capacitance versus output power at rated terminal voltage and rated speed

For constant terminal voltage/speed, the capacitance has to increase for an increase in the output power. The excitation capacitance in figure 4 and figure 5 is limited to 28µf. This is to avoid the operation in saturation. Figure 7 illustrates that the excitation capacitance has to increase by around 60% for 50% increase in the load power. Again, the results in figure 7 concur with the conclusions in Section 19.6 in [1].

VII. VERSATILITY OF THE DERIVED FORMULAS

The ability of proposed expressions to determine the critical excitation capacitance for other machines was investigated. The critical excitation capacitance for a number of induction generators with different power levels are estimated by the advised formulas and PSO Two examples are given below; the minimum capacitance for 1.1kW, [16] and 373kW, [2], are

shown in figure 8 and figure 9. The parameters of these machines are given in the Appendix in Tables III and IV for 1.1kW and 373kW respectively. The magnetization curves (B-H) for these machines are given in references [2] for 373kW and [16] for 1.1kW. It is worth to mention that magnetizing reactance's used for developing figure 3, figure 8 and figure 9 are corresponding to edge between saturation and un-saturation zones in (B-H) curves. This is to simplify the analysis. However, for investigating the steady-state performance of 3.7kW, values of magnetizing reactance are obtained from Fig. 2 and from optimization. The critical excitation capacitance for 1.1kW and 373kW are computed for wide range of speed from 0.7 to 1.4pu, as in figure 3.

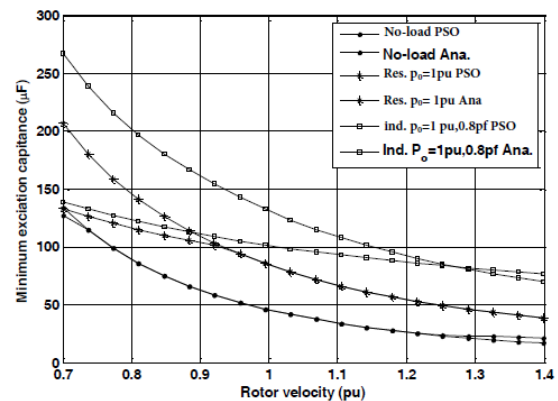


Fig. 8. Critical capacitance with rotor speed for No-load (dots), resistive load at rated power (stars), inductive load at rated power and 0.8pf lag (squares) from analytical expressions (dashed line), PSO solid line for 1.1kW machine

Again good correlation between results from the advised formulas and PSO is illustrated in Fig. 8, particularly for the no- load and resistive load scenarios. Comparing Figs. 3 and 8 reveals that excitation capacitance varies noticeably with magnetizing reactance. Moreover, as mentioned before, the minimum capacitance could be considered as speed dependent, figure 3 and 8. It is worth to mention that the deviation between the results from PSO and the derived equations is attributed to the constraints on independent variables.

Comparing figure 8 and figure 4 in ref. [16] validates the derived expressions here; as high degree of resemblance is obvious between these two figures. To expose the similarity of the results from the proposed formulas here and those from numerical techniques in [16], a number of minimum capacitance values are given in table II.

Table II shows that the results have significant correlation for no-load case. For resistive and inductive loads, the derived expressions here give slightly small regarding to [16]. This may be attributed to the value of the magnetizing reactance. As mentioned before that ref. [16] utilize a numerically interactive method based on eigenvalues, which could not identified explicitly the influence of different machine and load parameters on the value of the critical capacitance. In the contrary the expressions proposed here, equations (3), (6), and (8) ,show explicitly the role of different parameters

in the capacitor value. This is useful tool for the design and the operation of the SEIG.

TABLE II. Critical excitation capacitance

Speed	Load	Minimum capacitance from derived expressions here	Minimum capacitance from [16]
0.8pu	No-load	78μF	79μF
1pu	No-load	48.3μF	49.5 μF
1pu	1pu	94μF	112μF
1.1pu	1pu	79μF	98μF
1pu	1pu at	130μF	136μF

TABLE III. Parameters of 1.1KW IG [16]

Line voltage	220V
Number of poles	2
Frequency	60Hz
Stator resistance R_s (p.u.)	0.0946 p.u
Rotor resistance referred to the stator R_r (p.u)	0.0439 p.u
Stator leakage reactance X_{Ls} (p.u)	0.0865 p.u
Rotor resistance referred to the stator X_{Lr} (p.u)	0.0865 p.u

TABLE IV. Parameters of 373KW machine [2]

Line voltage	2300
Number of poles	2
Frequency	50Hz
Stator resistance R_s (p.u.)	0.0185p.u
Rotor resistance referred to the stator R_r (p.u)	0.0132 p.u
Stator leakage reactance X_{Ls} (p.u)	0.0850 p.u
Rotor resistance referred to the stator X_{Lr} (p.u)	0.0850 p.u

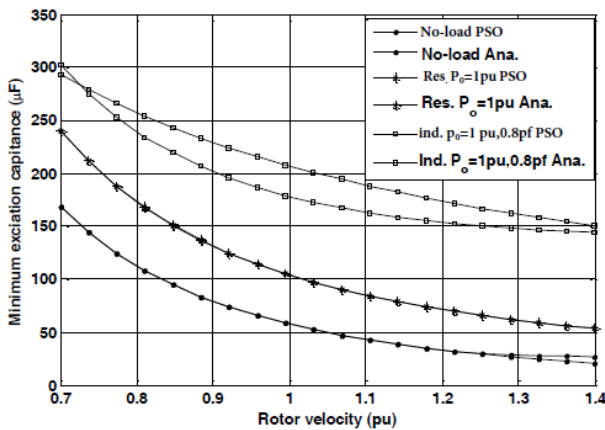


Fig. 10. Capacitive reactance (pu) for 373kW (dotted), 3.7kW (asterisks) and 1.1kW (squares) for full load at 0.707pf lag versus rotor velocity (pu)

Figure 10 shows that for full load at 0.707 pf lag, the 373kW machine has highest pu capacitive reactance over the entire speed range; while 1.1kW has the lowest pu captive reactance. This is possibly attributed to the limits imposed in generating frequency.

VIII. CONCLUSION

The following conclusions can be drawn:

1. The IG seems to be the preferred option for harvesting electrical power from renewable energy sources, due to its salient advantages: robustness, maintenance free and reduced volumetric dimension/cost.

2. Capacitor banks are mandatory for stand-alone operation of SEIG for supplying the machine with reactive power requirements, (5).
3. Analytical expressions were derived for minimum capacitance and generated frequency for different load types. These formulas show explicitly the parameters that affected the critical capacitance and the generated frequency. The minimum capacitor varies nearly inversely with the square of the rotor speed. The generated frequency drops with the load increase, while excitation capacitance increases.
4. A good correlation between the results from the derived expressions, PSO and the test-rig.
5. The terminal voltage of IG increases/decreases with increase/reduction in the output capacitance
6. For constant terminal voltage and speed, the excitation capacitance has to vary with the load.
7. The performance of self-excited induction generator is investigated here for different loads/operating conditions, which is likely novel.
8. The advised expressions are validated for generators with different sizes/ratings by comparing the results with those obtained from PSO for such machines. This confirms the effectiveness, robustness and feasibility of these formulas.
9. The proposed analytical expressions here and the presented results concur with the reported in literature, as in [1] and [16].

APPENDIX

$$Z_s = \frac{R_s}{F} + jX_L, Z_r = \frac{R_r}{F-v} + jX_{Lr}, Z_m = jX_m, Z_c = -j\frac{X_c}{F^2}$$

$$\text{and } Z_L = \frac{R_L}{F} + jX_L$$

The coefficients of equation (11)

$$a_1 = -((2X_m+X_L) X_L R_L + X_L^2 (X_L+X_m) (R_r+R_s))$$

$$a_2 = (2X_m+X_L) X_L R_L v + R_s X_L (X_L+X_m) v$$

$$a_3 = (R_L + R_s + R_r) (X_m+X_L) + (X_L R_L), a_4 = R_s R_L R_r$$

$$a_5 = - (R_s+R_L) (X_m+X_L) v$$

The coefficients of equation (12)

$$b_1 = -X_L X_L (X_L+2X_m), b_2 = -X_L X_L (X_L+2X_m) v$$

$$b_3 = (X_m+X_L) (X_L+X_L) + (X_L X_m)$$

$$b_4 = R_s X_L R_r + R_L (X_m+X_L) (R_s+R_r)$$

$$b_5 = -((X_m+X_L) (X_L+X_L) + X_L X_m) v$$

$$b_6 = -R_s R_L (X_m+X_L) v, b_7 = -R_r (R_s+R_L)$$

The coefficients of equation (15)

$$c_1 = -X_L (R_s+R_r) - (2X_L) R_L, c_2 = -X_L X_L (R_s+R_r) - (X_2) R_L$$

$$c_3 = (2X_L R_L v + R_s X_L v), c_4 = X_L (R_s X_L v + X_L R_L v)$$

$$c_5 = X_c (R_L+R_s+R_r), c_6 = X_L X_c R_r + R_s R_L R_r + X_L X_c (R_L+R_s+R_r)$$

$$c_7 = -X_c (R_L+R_s) v, c_8 = -X_L X_c (R_L+R_s) v;$$

The coefficients of equation (16)

$$d_1 = -2X_L X_L, d_2 = -X_L (X_L^2), d_3 = 2X_L X_L v$$

$$d_4 = (X_L^2) X_L v, d_5 = (R_s R_L + 2X_L X_c + X_L X_c + R_r R_L)$$

$$d_6 = X_L (R_s R_r + X_c X_L) + (X_L R_L) (R_r+R_s) + (X_2) X_c$$

$$d_7 = v ((-2X_L X_c) - (R_s R_L) - (X_c X_L))$$

$$d_8 = X_L v (-R_s R_L - X_L X_c - X_c X_L), d_9 = -X_c R_r (R_s+R_L)$$

REFERENCES

- [1] Bodlea and S. A. Nassar, *Induction machine handbook*, Second Edition, CRC press, 2010.
- [2] P. C. Krause, O. Wasynczuk, and S. D. Sudhoff, *Analysis of Electric Machinery*, IEEE Press, 1994.
- [3] R. C. Bansal, "Three-phase self-excited induction generators: an overview," *IEEE Transaction on Energy Conversion*, vol. 20, no. 2, pp. 292-299, 2005.
- [4] S. Boora, "On-set theory of self-excitation in induction generator," *International Journal of Recent Trends in Engineering*, vol. 2, no. 5, pp. 213-219, 2009.
- [5] S. Mahley, "Steady state analysis of three-phase self-excited induction generator," M. Sc. Thesis, Thapar University, Patiala, 2008.
- [6] H. Amimeur, R. Abdessemed, and E. Merabet, "Modeling and analysis of dual-stator windings self-excited induction generator," *Journal of Electrical Engineering (JEE)*, vol. 8, no. 3, pp. 18-24, 2008.
- [7] Y. J. Wang and S. Y. Huang, "Analysis of a self-excited induction generator supplying unbalanced load," *International Conference on Power System Technology*, vol. 2, pp. 1457-1462, 2004.
- [8] S. S. Murthy, O. P. Malik, and A. K. Tandon, "Analysis of self excited induction generators," *Proceeding of IEE*, vol. 129, pp. 260-265, 1982.
- [9] N. H. Malik and A. A. Mazi, "Capacitance requirements for isolated self excited induction generators," *IEEE Transactions on Energy Conversion*, vol. EC-2, pp. 62-69, 1987.
- [10] A. K. Tandon, S. S. Murthy, and G. J. Berg, "Steady state analysis of capacitor self excited induction generators," *IEEE Transactions on Power Apparatus and Systems*, vol. PAS-103, no. 3, pp. 12-618, 1984.
- [11] A. K. AL- Jabri and A. I. Alolah, "Capacitance requirement for isolated self – excited induction generator," *Proceeding IEE*, vol. 137, pp. 154-159, 1990.
- [12] A. K. AL- Jabri and A. I. Alolah, "Limits on the performance of three self excited induction generators," *IEEE Transactions on Energy Power Conversion*, vol. 5, pp. 350–356, 1990.
- [13] N. H. Malik, A. H. AL- Bahrani, "Influence of terminal capacitor on the performance characteristics of a self – excited induction generator," *IEE*, vol. 137, pp.168 -173, 1990.
- [14] S. P. Singh, B. Singh, and M. P. Jain, "Performance characteristics and optimum utilization of a cage machine as capacitor excited induction generator," *IEEE Transactions on Energy Power Conversion*, vol. 5, pp. 679–685, 1990.
- [15] M. H. Haque, "A novel method of evaluating performance characteristics of a self-excited induction generator," *IEEE Transactions on Energy Power Conversion*, vol. 24, pp. 358–365, 2009.
- [16] L. Wang and C. Huei, "A novel analysis on the performance of an isolated self-excited induction generator," *IEEE Transactions on Energy Power Conversion*, vol. 12, no. 2, pp. 109-117, 1997.
- [17] R. Ali, A. A. Abdelhafez, and G. El Sady, "Performance optimization of self-excited induction generator using simulated annealing technique," *Journal of Electrical Engineering, JEE*, vol. 1, 2012
- [18] S. N., Mahato, P. S. Singh, and M. P. Sharma, "Capacitors required for maximum power of a self-excited single-phase induction generator using a three-phase machine," *IEEE Transactions on Energy Conversion*, vol. 23, no. 2, pp. 372-381, 2008.
- [19] M. H. Haque and A. I. Maswood, "Determination of excitation capacitance of a three-phase self-excited induction generator," *IEEE Power and Energy Society General Meeting*, pp. 1-6, 2012.
- [20] S. P. Singh, B. Singh, and M. P. Jain, "A new technique for the analysis of excited induction generator," *IEEE Transactions on Energy Power Conversion*, vol. 23, pp. 647–656, 1993.
- [21] N. H. Malik and S. E. Haque, "Steady state analysis and performance of an isolated self-excited induction generator," *IEEE Transactions on Energy Conversion*, vol. EC-1, no. 3, pp. 134-140, 1986.
- [22] S. R. Singiresu, *Engineering Optimization Theory and Practice*, New Jersey: John Wiley & Sons, pp. 708, 2009.